Published in final edited form as:
J Cell Sci. 2008 April 15; 121(0 8): 1243–1251. doi:10.1242/jcs.017517.

Recycling of IRAP from the plasma membrane back to the insulin-responsive compartment requires the Q-SNARE syntaxin 6 but not the GGA clathrin adaptors

Robert T. Watson and **Jeffrey E. Pessin***
Department of Pharmacological Sciences, Stony Brook University, Stony Brook, NY 11794, USA

Summary

Insulin recruits two transmembrane proteins, GLUT4 and IRAP, to the plasma membrane of muscle cells and adipocytes. The subcellular trafficking and localization of GLUT4, and to a lesser extent IRAP, have been intensely studied, yet the molecular mechanisms responsible for their insulin-responsive compartmentalization remain unknown. Herein we have investigated the endocytosis and recycling of IRAP from the cell surface back to the insulin-responsive compartment (IRC). Our results show that a key dileucine motif at position 76,77 ($LL^{76,77}$), although required for the initial biosynthetic entry of IRAP into the IRC, is dispensable for entry into the IRC via the endosomal system. Indeed, we found that an $AA^{76,77}$ mutant of IRAP is fully capable of undergoing endocytosis and is correctly routed back to the IRC. To verify that the $AA^{76,77}$ mutant enters the bona fide IRC, we show that the internalized IRAP-$AA^{76,77}$ construct is sequestered in an IRC that is insensitive to brefeldin A yet sensitive to a dominant-interfering mutant of AS160 (AS160-4P). In addition, we show that the GGA clathrin adaptors are not required for the re-entry of IRAP from the cell surface back into the IRC, whereas the Q-SNARE syntaxin 6 is required for this process.

Keywords

IRAP; Insulin; AS160; Syntaxin 6; GGA; GLUT4

Introduction

The insulin-responsive aminopeptidase (IRAP) was originally identified in adipocytes as a 160-kDa type 2 integral membrane protein that co-fractionated with the insulin-responsive glucose transporter GLUT4 (Kandror and Pilch, 1994b; Kandror et al., 1994). Subsequently identified as the placental leucine aminopeptidase (P-LAP), IRAP is a member of the zinc-dependent membrane aminopeptidase family (Keller, 2003). In addition to a short cytoplasmic tail region and a single transmembrane domain, IRAP has a large extracellular region that contains the catalytic and zinc-binding domains (Keller, 2004). IRAP is known to cleave a number of small peptides, including vasopressin, angiotensins III and IV, and oxytocin, among others, under in vitro conditions (Keller, 2003). Thus, IRAP could function

*Author for correspondence (jpessin@aecom.yu.edu).

in the processing of circulating peptide hormones, although its in vivo substrates remain unknown. IRAP knockout mice have recently been generated, and although the *IRAP*$^{-/-}$ animals showed normal growth rates and were not diabetic, the total amount of GLUT4 protein was reduced by 50–80% in the major insulin-responsive tissues, i.e. striated muscle and adipose tissue (Keller et al., 2002). In addition, the genetic ablation of GLUT4 altered the subcellular distribution and expression levels of the IRAP protein (Abel et al., 2004; Carvalho et al., 2004). These data suggest a functional relationship between IRAP and GLUT4; however, a molecular mechanism has not been elucidated.

GLUT4 is expressed predominantly in muscle and adipose tissues, the major sites of postprandial glucose disposal (Bryant et al., 2002; Watson et al., 2004a). By contrast, IRAP shows broad tissue distribution (Keller, 2003). However, IRAP displays subcellular compartmentalization and insulin-stimulated trafficking properties that are indistinguishable from those of GLUT4 in both adipocytes and muscle cells (Kandror and Pilch, 1994a; Kandror and Pilch, 1994b; Kandror et al., 1994; Ueyama et al., 1999). In the basal state, both GLUT4 and IRAP cycle slowly to and from the plasma membrane (PM), with the vast majority of both proteins colocalizing within internal membrane compartments. Insulin stimulation causes the rapid redistribution of IRAP/GLUT4 to the cell surface, primarily by accelerating exocytosis with a relatively small decrease in the rate of PM endocytosis (Huang and Czech, 2007; Kanzaki, 2006).

It is well-established that the activated insulin receptor phosphorylates a number of substrate molecules, notably the insulin receptor substrate (IRS) proteins (Watson and Pessin, 2006). Tyrosine-phosphorylated IRS proteins provide docking sites for several downstream effectors, but the most important regarding glucose transport is arguably the Type 1A phosphatidylinositol 3′-kinase (Dugani and Klip, 2005). This enzyme generates phosphatidylinositol (3,4,5)-trisphosphate [PtdIns(3,4,5)P_3] in the membrane, which in turn recruits and activates the serine/threonine kinases PDK1, atypical PKCs and Akt (Czech, 2003; He et al., 2007). Recent work has identified a new downstream target of Akt, called AS160. In the relatively brief period since its initial identification (Sano et al., 2003), AS160 has generated substantial interest because it harbors a Rab GAP (GTPase-activating protein) domain that might participate in regulating one or more steps of IRAP/GLUT4 trafficking (Arias et al., 2007; Bruss et al., 2005; Eguez et al., 2005; Ishikura et al., 2007; Kramer et al., 2006; Larance et al., 2005; Miinea et al., 2005; Peck et al., 2006; Ramm et al., 2006; Sano et al., 2007; Sano et al., 2003; Thong et al., 2007).

The subcellular trafficking and localization of GLUT4, and to a lesser extent IRAP, have been intensely studied, yet the molecular mechanisms responsible for their insulin-responsive compartmentalization remain unknown (Holman and Sandoval, 2001; Keller, 2003). The GLUT4 protein has a complicated structure with 12 transmembrane domains and seven discrete cytoplasmic regions that could, collectively or individually, contribute sorting information (Lalioti et al., 2001). Although GLUT4 and IRAP show indistinguishable trafficking properties, IRAP is a type 2 transmembrane protein with a single 109-aminoacid cytoplasmic tail region that encodes all the necessary sorting information for insulin-responsive compartmentalization (Johnson et al., 2001; Lampson et al., 2000; Subtil et al., 2000). IRAP is therefore an excellent tool for elucidating how adipocytes compartmentalize

insulin-responsive transmembrane proteins. Indeed, similar to GLUT4, we recently found that the Golgi-localized, γ-ear-containing, Arf (ADP-ribosylation factor)-binding (GGA) family of clathrin adaptors is required to sort newly synthesized IRAP from the trans-Golgi network (TGN) into the insulin responsive compartment (IRC) (Hou et al., 2006; Liu et al., 2005). In the present study, we investigated the role of GGA adapters, AS160 and syntaxin 6 (Stx6) in the recycling of IRAP from the cell surface back to the IRC.

Results

The cytosolic, N-terminal tail region of IRAP consists of 109 amino acids and encodes all the necessary information for correct insulin-responsive compartmentalization (Hou et al., 2006). For example, when the cytosolic tail of IRAP is grafted onto the transmembrane and extracellular domains of the transferrin receptor (TfR), the resulting heterologous chimera (IRAP-TfR) traffics in a manner indistinguishable from IRAP and GLUT4 (Hou et al., 2006; Johnson et al., 2001; Lampson et al., 2000; Subtil et al., 2000). Using the IRAP-TfR reporter construct, we recently reported on the characterization of a dileucine motif at position 76,77 that is required to sort IRAP into the IRC following its initial biosynthesis (Hou et al., 2006). When this critical dileucine motif was mutated to alanine residues (IRAP-TfR-AA^{76,77}), the resulting construct rapidly defaulted to the PM in a manner indistinguishable from other constitutive trafficking proteins, including the newly synthesized transferrin receptor itself, VSV-G protein, Stx3 and GLUT1 (Hou et al., 2006) (Fig. 1A,B). In addition, correct sorting of newly synthesized wild-type IRAP requires the GGA clathrin adaptors, which function at the level of the TGN to sort IRAP into the IRC (Hou et al., 2006). By contrast, IRAP-TfR-AA^{76,77} bypasses the GGA sorting machinery and defaults to the PM, demonstrating that the IRAP-TfR-AA^{76,77} construct is misrouted to the constitutive exocytic pathway prior to the GGA-dependent sorting step (Hou et al., 2006). However, it remains unclear whether the observed cell-surface accumulation of IRAP-TfR-AA^{76,77} is due to the rapid default of the construct to the PM, or an impairment of endocytosis, or perhaps a combination of the two. To address this issue, we transfected adipocytes with the *IRAP-TfR*-AA^{76,77} construct, and after an overnight recovery period, incubated the cells without or with 10 μM cycloheximide to inhibit new protein synthesis (Fig. 1C–E). In control cells treated with vehicle alone, we observed no change in the cell-surface localization of the IRAP-TfR-AA^{76,77} reporter (Fig. 1Ca–d). However, in the presence of cycloheximide, we observed a rapid clearing of the reporter construct from the cell surface (Fig. 1Ce–h). Quantification of these results is shown in Fig. 1D and clearly demonstrates the loss of the PM-localized IRAP-TfR-AA^{76,77} in the presence of cycloheximide relative to vehicle controls over the 4-hour time course of the experiment. We next tested the stability of the IRAP-TfR-WT (wild-type IRAP) and IRAP-TfR-AA^{76,77} constructs (Fig. 1E). Fully differentiated 3T3L1 adipocytes were transfected with either *IRAP-TfR*-WT or *IRAP-TfR*-AA^{76,77} and allowed to recover overnight. Cells were then incubated for the indicated times in 10 μg/ml cycloheximide (Fig. 1E). In lane 1 in Fig. 1E, cells were immediately plated directly in cycloheximide following transfection, in order to test the effectiveness of the drug to inhibit translation. The upper panel in Fig. 1E shows endogenous IRAP, which displays no appreciable change in expression levels over the 6-hour time frame of the experiment. Similarly, both the IRAP-TfR-WT and IRAP-TfR-AA^{76,77} chimeras also showed no significant reduction in protein

expression levels over the 6-hour cycloheximide time course. We chose a 6-hour time frame for this experiment because our subsequent endocytosis assays were also performed over a 4- to 6-hour time period.

The above data suggest that the rapid default of newly synthesized IRAP-TfR-AA^{76,77} accounts for the steady-state distribution of the reporter at the PM, rather than an impairment in endocytosis. We therefore decided to examine the trafficking properties of the IRAP-TfR-AA^{76,77} mutant following its endocytosis from the cell surface (Fig. 2). This was accomplished by electroporating differentiated 3T3L1 adipocytes with either *IRAP-TfR*-WT or *IRAP-TfR*-AA^{76,77} cDNAs, allowing the cells to recover overnight and stimulating with 100 nM insulin to achieve maximal recruitment of both constructs to the cell surface. The cells were then incubated on ice and surface-labeled with an exofacial anti-TfR antibody for 60 minutes. After washing three times with ice-cold PBS, the cells were warmed to 37°C for various times, fixed and labeled with Texas Red secondary antibody, as described in the Materials and Methods section. Fig. 2A shows a representative time course for endocytosis of the wild type and AA^{76,77} constructs. Quantification of the ratio of cell-surface to total-cell fluorescence was achieved using the Zeiss LSM software package (Fig. 2B). As is readily apparent, the IRAP-TfR-AA^{76,77} mutant was fully capable of undergoing PM endocytosis in a manner indistinguishable from that of IRAP-TfR-WT. We next determined whether the surface-internalized IRAP-TfR-AA^{76,77} construct colocalized with GLUT4 in the perinuclear region (Fig. 2C). Fully differentiated 3T3L1 adipocytes were co-transfected with HA-*GLUT4* and *IRAP-TfR*-AA^{76,77}, and allowed to recover overnight. Cells were then stimulated with insulin for 20 minutes, cooled on ice, and surface-labeled with rabbit anti-HA and mouse anti-TfR antibodies, following the same protocol as described above. At the *t*=0 time point, we observed extensive cell-surface labeling of both HA-GLUT4 and IRAP-TfR-AA^{76,77}. After three washes with ice-cold PBS, cells were warmed to 37°C for 6 hours to allow endocytosis to occur. Following endocytosis, we observed substantial overlap between HA-GLUT4 and IRAP-TfR-AA^{76,77} in the perinuclear region, as well as in a subset of cytosolic punctuate structures.

Together, the above data show that newly synthesized IRAP-TfR-AA^{76,77} rapidly defaults to the PM, but once at the cell surface, this construct undergoes efficient endocytosis. We therefore examined the ability of the IRAP-TfR-AA^{76,77} construct to recycle from the cell surface back to the IRC (Fig. 3A). A well-known property of the IRC is that it is insensitive to the fungal metabolite brefeldin A (BFA) (Bao et al., 1995; Chakrabarti et al., 1994; Kono-Sugita et al., 1996; Liu et al., 2005; Martin et al., 2000; Palacios et al., 2001), which inhibits a subset of ADP-ribosylation factor (ARF) isoforms (Chardin and McCormick, 1999; Klausner et al., 1992). Thus, if the IRAP-TfR-AA^{76,77} construct is correctly routed from the cell surface to the IRC, then it should be capable of undergoing a second round of insulin-stimulated translocation, even in the presence of BFA. To test this hypothesis, we electroporated adipocytes with either *IRAP-TfR*-WT or *IRAP-TfR*-AA^{76,77}, allowed the cells to recover overnight and then stimulated them with 100 nM insulin to maximally recruit both reporter constructs to the cell surface. After labeling the cell surface with the anti-TfR antibody on ice, cells were warmed to 37°C for 3.5 hours and then treated with or without 5 μg/ml BFA for an additional 30 minutes. Cells were then stimulated with or without 100 nM

insulin in the presence or absence of 5 μg/ml BFA (Watson and Pessin, 2000), fixed and labeled with Texas-Red-conjugated secondary antibody. As shown in Fig. 3A, we observed that ~80% of the fluorescence signal was present at the cell surface at time *t*=0. After the 4-hour washout, ~10–15% of the fluorescence signal was at the PM, indicating efficient endocytosis of both the IRAP-TfR-WT and IRAP-TfR-AA^{76,77} constructs. Following insulin stimulation, ~40–45% of the fluorescence signal returned to the cell surface, indicating recruitment of IRAP-TfR-WT and IRAP-TfR-AA^{76,77} to the PM. We consistently observed that, following insulin stimulation, ~40–50% of the *t*=0 fluorescence value returned to the PM, similar to what has been previously reported using an exofacial bismannose photolabeling approach to study GLUT4 recycling (Satoh et al., 1993). These data show that the IRAP-TfR-AA^{76,77} construct undergoes efficient endocytosis and is routed to an insulin-responsive subcellular compartment. Furthermore, we observed that both IRAP-TfR-WT and IRAP-TfR-AA^{76,77} were fully capable of undergoing a second round of insulin-stimulated translocation, even in the presence of 5 μg/ml BFA, consistent with the known properties of the bona fide IRC (Bao et al., 1995; Kono-Sugita et al., 1996; Martin et al., 2000; Satoh et al., 1993). Fig. 3B shows control experiments demonstrating the efficacy of the 5 μg/ml BFA treatment. For these experiments, a GFP-IRAP-AA^{76,77} reporter was used, because this construct is known to default to the cell surface immediately following its initial biosynthesis (Hou et al., 2006). Cells were transfected with the *GFP-IRAP*-AA^{76,77} reporter and immediately plated in media either without (Fig. 3Ba–c) or with (panels d–f) 5 μg/ml BFA. After a 3-hour recovery period, cells were fixed and labeled with an anti-p115 (Golgi marker) monoclonal antibody, followed by Texas-Red-conjugated secondary antibodies. In the BFA-treated cells, newly synthesized GFP-IRAP-AA^{76,77} failed to localize to the PM, and the cis-Golgi marker p115 showed a dispersed expression pattern, consistent with BFA-induced disruption of Golgi structure and function.

Over the past several years, a new Akt substrate, AS160, has emerged as an important regulator of insulin-stimulated GLUT4 translocation (reviewed in Dugani and Klip, 2005; Huang and Czech, 2007; Jessen and Goodyear, 2005; Watson and Pessin, 2006). AS160 contains a Rab GAP domain and is thought to be a negative regulator of GLUT4 translocation in the absence of insulin (Eguez et al., 2005; Kramer et al., 2006; Miinea et al., 2005; Sano et al., 2007; Sano et al., 2003; Thong et al., 2007). Phosphorylation by Akt might abrogate the GAP activity of AS160, although the mechanism for this remains unclear. Originally cloned using a phospho-Akt substrate antibody, AS160 harbors six consensus Akt-phosphorylation sites (Sano et al., 2003). When four of these sites were mutated to alanines, the resulting construct (designated AS160-4P) behaved in a dominant-interfering manner to inhibit insulin-stimulated GLUT4 translocation (Sano et al., 2003). Since its original description, the AS160-4P construct has been employed by several groups to study GLUT4 trafficking dynamics under steady-state conditions (Eguez et al., 2005; Kramer et al., 2006; Miinea et al., 2005; Sano et al., 2007; Thong et al., 2007). In addition, AS160 has recently been reported to interact with IRAP (Peck et al., 2006; Ramm et al., 2006), and we have therefore used the AS160-4P construct to investigate the recycling properties of IRAP (Fig. 4). Fully differentiated 3T3L1 adipocytes were co-transfected with *IRAP-TfR*-AA^{76,77} and either *AS160*-WT or *AS160-4P*. After an overnight recovery period, cells were cooled on ice and surface-labeled with the anti-TfR antibody, as described for

Fig. 2. Following a washout period of 5.5 hours, cells were treated without or with 100 nM insulin for 30 minutes and processed for imaging by confocal microscopy. The ratio of PM to total fluorescence was determined and, as shown in Fig. 4, the AS160-4P construct had no significant effect on the biosynthetic accumulation of IRAP-TfR-AA^{76,77} at the PM. However, following endocytosis, the AS160-4P protein inhibited the ability of insulin to stimulate translocation, whereas the AS160-WT construct was without effect. These data provide an additional level of confirmation that the IRAP-TfR-AA^{76,77} construct recycles back to the IRC and, subsequently, undergoes a normal extent of insulin-stimulated translocation.

We next took advantage of the recycling properties of IRAP-TfR-AA^{76,77} to examine the potential role of GGA in the endocytosis of IRAP and its recycling back to the IRC (Fig. 5). Previously, it was reported that GGA proteins function at the TGN during the entry of GLUT4 into the IRC (Watson et al., 2004b). By contrast, it was reported that GGA also functions in the recycling of GLUT4 from the PM back into the IRC (Li and Kandror, 2005). We previously showed that IRAP-TfR-AA^{76,77} defaults to the cell surface in the presence of the dominant-interfering GGA construct VHS-GAT [Vps27, Hrs, Stam, GGA and target of myb (TOM)] (Hou et al., 2006). Thus, based upon the above and established trafficking properties of IRAP-TfR-AA^{76,77}, this construct provides an experimental tool to distinguish these two trafficking steps. To determine whether GGA adaptors function during the endocytosis and recycling of IRAP, fully differentiated 3T3L1 adipocytes were co-transfected with 50 μg of *IRAP-TfR*-AA^{76,77} and 200 μg of either *GGA*-WT or the *VHS-GAT* construct (Fig. 5). After an overnight recovery period, cells were cooled on ice and surface-labeled with the anti-TfR antibody for 60 minutes, as described for Fig. 2. Cells were then washed three times in ice-cold PBS and warmed to 37°C for various times. As shown in Fig. 5A, we observed no measurable difference in the endocytosis kinetics of the IRAP-TfR-AA^{76,77} reporter in the presence of co-expressed GGA-WT versus VHS-GAT. In addition, the IRAP-TfR-AA^{76,77} reporter was fully capable of undergoing a second round of insulin-stimulated translocation in the presence of the VHS-GAT construct, and this response was indistinguishable from cells co-expressing the GGA-WT construct (Fig. 5B). Together, these data support a model wherein GGA adaptors are not required for the endocytosis and routing of IRAP from the cell surface back the IRC; rather, the GGA adaptors appear to function specifically at the TGN during the biosynthetic entry of IRAP into the IRC.

Having established a paradigm to distinguish between proteins required for the biosynthetic sorting and PM recycling into the IRC, we next applied this approach to examine the properties of a Q-SNARE protein, Stx6, which is thought to participate in membrane-fusion events at the TGN and endosome compartments (Bock et al., 1997; Bock et al., 1996; Klumperman et al., 1998; Kuliawat et al., 2004; Murray et al., 2005; Perera et al., 2003; Shewan et al., 2003; Simonsen et al., 1999; Steegmaier et al., 1999; Wang et al., 2005; Watson and Pessin, 2000; Wendler et al., 2001). Q-SNAREs harbor key glutamine residues and are distinguished from R-SNAREs, which contain a key arginine residue (Jahn and Scheller, 2006). As shown in Fig. 6, transfection with a *Stx6*-specific siRNA effectively reduced Stx6 protein expression at 72 hours (Fig. 6A) and 96 hours (Fig. 6B) post-transfection compared with a scrambled siRNA. This occurred without affecting the

expression of other related Q-SNARE molecules, including Stx4 and Stx16. To test the potential role of Stx6 in IRAP trafficking, we next co-transfected siRNAs directed against *Stx6* with the *IRAP-TfR*-AA^{76,77} reporter (Fig. 6C). Adipocytes were first transfected with 5 nmol of scrambled or *Stx6* siRNA and, 72 hours later, were transfected a second time with the *IRAP-TfR*-AA^{76,77} reporter. The cells were allowed to recover for 18 hours and were then surface-labeled with the anti-TfR antibody for 60 minutes on ice. After a 5.5-hour washout period at 37°C, cells were incubated without or with 100 nM insulin for 30 minutes and processed for confocal microscopy. This protocol allows us to achieve efficient knockdown of Stx6 prior to the expression of the IRAP reporter construct (Hou et al., 2006). In the presence of scrambled siRNA, the IRAP-TfR-AA^{76,77} reporter was fully capable of internalizing from the cell surface and undergoing a second round of insulin-stimulated translocation. By contrast, in Stx6 knockdown cells, the IRAP-TfR-AA^{76,77} reporter was efficiently internalized from the PM but was unable to undergo a second round of insulin-stimulated exocytosis (Fig. 6C).

The results in Fig. 6 indicate that Stx6 plays a role in insulin-stimulated IRAP translocation, but it is unclear whether Stx6 functions during the insulin-stimulated exit of IRAP from the IRC or, alternatively, during the endosomal sorting and routing of IRAP from the PM back into the IRC. To distinguish between these possibilities, we used the IRAP-TfR-WT reporter, which we have previously shown is directly sorted from the Golgi into the IRC, without first traversing the PM (Hou et al., 2006). Adipocytes were first transfected with 5 nmol of scrambled or *Stx6* siRNA and, 72 hours later, were transfected with the *IRAP-TfR*-WT reporter. The cells were allowed to recover for 24 hours, and were then stimulated without or with 100 nM insulin and processed for confocal microscopy. Using this methodology, we observed no impairment in the insulin-stimulated translocation of the IRAP reporter (Fig. 7A). We therefore next tested whether Stx6 knockdown had any effect on the recycling of IRAP from the cell surface back into the IRC (Fig. 7B). To address this question, we first transfected adipocytes with *Stx6* siRNA and then, 72 hours later, cells were transfected again with *IRAP-TfR*-WT. Following an 18-hour recovery period, cells were stimulated with insulin to recruit the IRAP reporter to the PM, and were then incubated on ice and surface-labeled with the anti-TfR antibody for 60 minutes. Cells were then washed with ice-cold PBS and warmed to 37°C for 5.5 hours. They were then stimulated without or with 100 nM insulin for 30 minutes and processed for confocal microscopy. As shown in Fig. 7B, Stx6 knockdown significantly impaired the ability of surface-internalized IRAP-TfR-WT to undergo a second round of insulin-stimulated translocation. Together, these data suggest that Stx6 function, in contrast to GGA, is required for the recycling of IRAP from the cell surface back into the IRC, but not for the insulin-stimulated recruitment of IRAP from the IRC to the PM.

Discussion

In the present study, we took advantage of the comparatively simple molecular architecture of the IRAP protein to elucidate cis-sequence motifs and trans-acting proteins that function during its trafficking from the cell surface back to the IRC. Unlike wild-type IRAP, the AA^{76,77} mutant bypasses the IRC and defaults to the PM following its initial biosynthesis (Hou et al., 2006). We show here, however, that, once at the PM, this mutant undergoes

endocytosis, sorts back into the IRC and is fully capable of another round of insulin-stimulated translocation. Although unlikely, it is formally possible that the IRAP-TfR-AA^{76,77} mutant undergoes normal endocytosis and subsequent insulin-stimulated translocation despite having recycled to different intracellular compartments that are insulin responsive but distinct from the storage compartment used by endogenous IRAP/GLUT4. To address this important issue, we took several experimental approaches. First, the IRAP-TfR-AA^{76,77} and IRAP-TfR-WT constructs show indistinguishable trafficking properties following endocytosis from the cell surface, and both undergo similar extents of translocation following insulin stimulation. Second, the IRAP-TfR-AA^{76,77} construct recycles back to an IRC that is insensitive to BFA. BFA inhibits a subset of Arf isoforms and therefore disrupts many intracellular trafficking processes (Chardin and McCormick, 1999; Jackson and Casanova, 2000; Klausner et al., 1992), but the IRC is well-known to be refractory to BFA (Bao et al., 1995; Kono-Sugita et al., 1996; Martin et al., 2000; Satoh et al., 1993). Third, AS160-4P, a dominant-interfering mutant of AS160, binds to IRAP and is known to inhibit the insulin-stimulated recruitment of GLUT4 to the cell surface (Eguez et al., 2005; Kramer et al., 2006; Miinea et al., 2005; Ramm et al., 2006; Sano et al., 2007; Sano et al., 2003; Thong et al., 2007). Similarly, in the present study we also observed that AS160-4P inhibited the translocation of surface-internalized IRAP-TfR-AA^{76,77} to the PM. Together, these data strongly support the contention that IRAP-TfR-AA^{76,77} is internalized and sorted back to the same IRC that is occupied by endogenous IRAP/GLUT4.

We showed previously that the GGA family of monomeric clathrin adaptors function at the level of the TGN to sort newly synthesized GLUT4 and IRAP into the IRC (Hou et al., 2006; Watson et al., 2004b). Although our experiments focused specifically on sorting events at the TGN, it was recently reported that GGA adaptors might also function in the recycling of GLUT4 from the PM back to the IRC (Li and Kandror, 2005). However, these studies were performed in an isolated stable clone of 3T3L1 adipocytes expressing the dominant-interfering GGA mutant, VHS-GAT. To further address this issue, we took advantage of the IRAP-TfR-AA^{76,77} mutant, which defaults to the cell surface even in the presence of the VHS-GAT dominant-interfering GGA mutant (Hou et al., 2006). We found that the IRAP-TfR-AA^{76,77} construct was fully capable of undergoing endocytosis and recycling back to the IRC in the presence of overexpressed VHS-GAT, conditions that are established to inhibit the entry of wild-type IRAP into the IRC from the biosynthetic route (Hou et al., 2006). Together, these data strongly indicate that GGA adaptors function specifically at the TGN during the initial entry of newly synthesized IRAP into the IRC.

Continuing our investigations into the endocytosis and recycling dynamics of IRAP, we next examined the potential functional role of the Q-SNARE Stx6 in the routing if IRAP from the cell surface back to the IRC. Stx6 colocalizes with GLUT4 in the perinuclear storage compartment, and has previously been implicated in membrane-trafficking processes at the TGN and endosome compartments, including GLUT4 sorting and translocation (Perera et al., 2003; Shewan et al., 2003). For example, Perera et al. (Perera et al., 2003) overexpressed the cytosolic region of Stx6 and observed an increase in basal glucose transport and increased GLUT4 protein at the cell surface. However, overexpression of the cytosolic domain of a SNARE (soluble NSF attachment protein receptor protein) is problematic, because there is a substantial risk for non-specific effects due to inhibition of other, highly

related SNARE family members. Thus, we took the approach of knocking down the expression levels of Stx6 and we observed an impairment of surface-internalized IRAP to return to the IRC. These results suggest an endosomal-sorting defect in the absence of Stx6, consistent with results from Kuliawat et al. (Kuliawat et al., 2004), who observed an endosomal-trafficking defect when the Stx6 cytosolic domain was overexpressed. Our results are also consistent with some of the findings of Perera et al. (Perera et al., 2003), although we did not observe an inhibition of endocytosis when Stx6 was knocked down, as was reported by these authors when they overexpressed the cytosolic domain of Stx6. This discrepancy might reflect off-target effects of the overexpressed Stx6 cytosolic region. Importantly, we did not observe any defects in the initial insulin-stimulated recruitment of newly synthesized IRAP from the IRC to the PM in Stx6 knockdown cells, suggesting that Stx6 functions specifically during the sorting of IRAP from the PM back into the IRC.

In summary, our previous results demonstrated that the dileucine motif at position 76,77 is essential for sorting newly synthesized IRAP from the Golgi into the IRC (Hou et al., 2006). In the present work, we show that $LL^{76,77}$ is not required for the entry of surface-internalized IRAP into the IRC, indicating that distinct sorting motifs operate at different locations in the subcellular-trafficking itinerary of IRAP to direct IRAP into the IRC. Future work will be required to elucidate the specific motifs that operate during the recycling of IRAP from the PM back into the IRC. However, in addition to cis-sequence elements within IRAP, trans factors must also participate in the sorting of this protein, and we also show here that the GGA clathrin adaptors are not required for the entry of surface-internalized IRAP into the IRC, whereas Stx6 is required for this process. Future work will focus on other SNARE family members that participate in the sorting of IRAP and GLUT4 during their complex subcellular-trafficking itineraries.

Materials and Methods

Reagents, antibodies and clones

BFA and cycloheximide were purchased from Sigma and dissolved in methanol at stock concentrations of 5 and 10 mg/ml, respectively. The mouse anti-human TfR antibody was from Molecular Probes (now a subsidiary of Invitrogen). The p115 and Stx6 antibodies were from BD Transduction Labs; the Stx16 antibody was from Synaptic Systems; the Stx4 antibody was from Sigma. The *IRAP-TfR*-WT, *IRAP-TfR*-$AA^{76,77}$, *GGA*-WT and *VHS-GAT* clones were described previously (Hou et al., 2006); the AS160 and AS160-4P clones were also described previously (Sano et al., 2003). The *Stx6* siRNA (5′-GGAUUGUUUCAGAGAUGGATT-3′) and random siRNA (5′-CGUCCAUAUACCGGUUCUUUG-3′) were obtained from Ambion.

Cell culture and electroporation

3T3L1 pre-adipocytes were purchased from the American Type Culture Collection, and were cultured and differentiated as described previously (Watson and Pessin, 2000). Fully differentiated 3T3L1 adipocytes (typically 5–8 days after addition of differentiation media) were electroporated with plasmid DNA prepared by the CsCl purification method.

Electroporation was performed as previously described (Min et al., 1999), using 0.16 kV and 950 μF, and transfected cells were plated on collagen-coated coverslips.

Endocytosis assays

Following electroporation, adipocytes were allowed to recover overnight (~16 hours) and were then treated with 100 nM insulin for 30 minutes at 37°C. Cells were then cooled on ice and incubated with the anti-TfR antibody (2 ng/ml) for 60 minutes. Cells were then washed three times with ice-cold PBS and warmed to 37°C for various times to allow endocytosis to occur. Cells were then fixed in 4% paraformaldehyde/0.2% TX-100 for 10 minutes, blocked with 5% donkey serum and 1% BSA for 30 minutes and labeled with Texas-Red-conjugated secondary antibody (Jackson ImmunoResearch Labs) for 30 minutes at 37°C.

Quantification of the fluorescence signal at the cell surface versus the total-cell fluorescence was performed using the Zeiss LSM software package. Briefly, individuals cells were circumscribed with two curves (~0.5-μm apart) that were used to define the outside and inside of the PM. The total fluorescence signal from a given cell was then calculated as the average pixel intensity multiplied by the two-dimensional surface area of the cell. The fluorescence signal at the PM was similarly calculated, except that the surface area corresponded specifically to the PM, rather than the entire cell. We then divided the PM fluorescence by the total fluorescence. Note that we are using a cDNA that encodes the human TfR, and we are using an exofacial TfR antibody directed against the human TfR. This minimizes cross-reaction with endogenous TfR (the 3T3L1 cells are of mouse origin).

Stx6 knockdown by siRNA and IRAP trafficking assays

Two separate protocols were used to assess the potential role of Stx6 in IRAP trafficking. In the first protocol, 3T3L1 adipocytes were transfected with 5 nmol of either scrambled or *Stx6* siRNA. The cells were then allowed to recover for 72 hours, at which time the cells were transfected again with the *EGFP-IRAP-TfR* reporter and allowed to recover for an additional 24 hours prior to treatment without or with 100 nM insulin for 30 minutes. The cells were then fixed in 4% paraformaldehyde, labeled with Texas Red secondary antibody and processed for confocal microscopy. Translocation was determined by quantifying the ratio of surface:total fluorescence (Texas Red:EGFP) using the Zeiss LSM software as previously described (Khan et al., 2004). In the second protocol, 3T3L1 adipocytes were electroporated with 5 nmol of scrambled or *Stx6* siRNA and allowed to recover for 72 hours as above, and then transfected with the *IRAP-TfR* reporter. After an 18-hour recovery period, the cells were stimulated with 100 nM insulin and the cells were surface-labeled on ice with anti-TfR monoclonal antibody for 60 minutes. The cells were then washed three times with ice-cold PBS, warmed to 37°C for 5.5 hours and treated with or without 100 nM insulin for 30 minutes. Cells were then fixed with 4% paraformaldehyde/0.2% TX100 and labeled with Texas Red secondary antibody. The ratio of surface:total fluorescence was then determined using the Zeiss LSM software.

References

Abel ED, Graveleau C, Betuing S, Pham M, Reay PA, Kandror V, Kupriyanova T, Xu Z, Kandror KV. Regulation of insulin-responsive aminopeptidase expression and targeting in the insulin-responsive

vesicle compartment of glucose transporter isoform 4-deficient cardiomyocytes. Mol Endocrinol. 2004; 18:2491–2501. [PubMed: 15231875]

Arias EB, Kim J, Funai K, Cartee GD. Prior exercise increases phosphorylation of Akt substrate of 160 kDa (AS160) in rat skeletal muscle. Am J Physiol Endocrinol Metab. 2007; 292:E1191–E1200. [PubMed: 17179389]

Bao S, Smith RM, Jarett L, Garvey WT. The effects of brefeldin A on the glucose transport system in rat adipocytes. Implications regarding the intracellular locus of insulin-sensitive Glut4. J Biol Chem. 1995; 270:30199–30204. [PubMed: 8530430]

Bock JB, Lin RC, Scheller RH. A new syntaxin family member implicated in targeting of intracellular transport vesicles. J Biol Chem. 1996; 271:17961–17965. [PubMed: 8663448]

Bock JB, Klumperman J, Davanger S, Scheller RH. Syntaxin 6 functions in trans-Golgi network vesicle trafficking. Mol Biol Cell. 1997; 8:1261–1271. [PubMed: 9243506]

Bruss MD, Arias EB, Lienhard GE, Cartee GD. Increased phosphorylation of Akt substrate of 160 kDa (AS160) in rat skeletal muscle in response to insulin or contractile activity. Diabetes. 2005; 54:41–50. [PubMed: 15616009]

Bryant NJ, Govers R, James DE. Regulated transport of the glucose transporter GLUT4. Nat Rev Mol Cell Biol. 2002; 3:267–277. [PubMed: 11994746]

Carvalho E, Schellhorn SE, Zabolotny JM, Martin S, Tozzo E, Peroni OD, Houseknecht KL, Mundt A, James DE, Kahn BB. GLUT4 overexpression or deficiency in adipocytes of transgenic mice alters the composition of GLUT4 vesicles and the subcellular localization of GLUT4 and insulin-responsive aminopeptidase. J Biol Chem. 2004; 279:21598–21605. [PubMed: 14985357]

Chakrabarti R, Buxton J, Joly M, Corvera S. Insulin-sensitive association of GLUT-4 with endocytic clathrin-coated vesicles revealed with the use of brefeldin A. J Biol Chem. 1994; 269:7926–7933. [PubMed: 8132512]

Chardin P, McCormick F. Brefeldin A: the advantage of being uncompetitive. Cell. 1999; 97:153–155. [PubMed: 10219235]

Czech MP. Dynamics of phosphoinositides in membrane retrieval and insertion. Annu Rev Physiol. 2003; 65:791–815. [PubMed: 12518000]

Dugani CB, Klip A. Glucose transporter 4, cycling, compartments and controversies. EMBO Rep. 2005; 6:1137–1142. [PubMed: 16319959]

Eguez L, Lee A, Chavez JA, Miinea CP, Kane S, Lienhard GE, McGraw TE. Full intracellular retention of GLUT4 requires AS160 Rab GTPase activating protein. Cell Metab. 2005; 2:263–272. [PubMed: 16213228]

He A, Liu X, Liu L, Chang Y, Fang F. How many signals impinge on GLUT4 activation by insulin? Cell Signal. 2007; 19:1–7. [PubMed: 16919913]

Holman GD, Sandoval I. Moving the insulin-regulated glucose transporter GLUT4 into and out of storage. Trends Cell Biol. 2001; 11:173–179. [PubMed: 11306298]

Hou JC, Suzuki N, Pessin JE, Watson RT. A specific dileucine motif is required for the GGA-dependent entry of newly synthesized insulin-responsive aminopeptidase into the insulin-responsive compartment. J Biol Chem. 2006; 281:33457–33466. [PubMed: 16945927]

Huang S, Czech MP. The GLUT4 glucose transporter. Cell Metab. 2007; 5:237–252. [PubMed: 17403369]

Ishikura S, Bilan PJ, Klip A. Rabs 8A and 14 are targets of the insulin-regulated Rab-GAP AS160 regulating GLUT4 traffic in muscle cells. Biochem Biophys Res Commun. 2007; 353:1074–1079. [PubMed: 17208202]

Jackson CL, Casanova JE. Turning on ARF: the Sec7 family of guanine-nucleotide-exchange factors. Trends Cell Biol. 2000; 10:60–67. [PubMed: 10652516]

Jahn R, Scheller RH. SNAREs – engines for membrane fusion. Nat Rev Mol Cell Biol. 2006; 7:631–643. [PubMed: 16912714]

Jessen N, Goodyear LJ. Contraction signaling to glucose transport in skeletal muscle. J Appl Physiol. 2005; 99:330–337. [PubMed: 16036906]

Johnson AO, Lampson MA, McGraw TE. A di-leucine sequence and a cluster of acidic amino acids are required for dynamic retention in the endosomal recycling compartment of fibroblasts. Mol Biol Cell. 2001; 12:367–381. [PubMed: 11179421]

Kandror K, Pilch PF. Identification and isolation of glycoproteins that translocate to the cell surface from GLUT4-enriched vesicles in an insulin-dependent fashion. J Biol Chem. 1994a; 269:138–142. [PubMed: 8276787]

Kandror KV, Pilch PF. gp160, a tissue-specific marker for insulin-activated glucose transport. Proc Natl Acad Sci USA. 1994b; 91:8017–8021. [PubMed: 8058750]

Kandror KV, Yu L, Pilch PF. The major protein of GLUT4-containing vesicles, gp160, has aminopeptidase activity. J Biol Chem. 1994; 269:30777–30780. [PubMed: 7983006]

Kanzaki M. Insulin receptor signals regulating GLUT4 translocation and actin dynamics. Endocr J. 2006; 53:267–293. [PubMed: 16702775]

Keller SR. The insulin-regulated aminopeptidase: a companion and regulator of GLUT4. Front Biosci. 2003; 8:s410–s420. [PubMed: 12700100]

Keller SR. Role of the insulin-regulated aminopeptidase IRAP in insulin action and diabetes. Biol Pharm Bull. 2004; 27:761–764. [PubMed: 15187412]

Keller SR, Davis AC, Clairmont KB. Mice deficient in the insulin-regulated membrane aminopeptidase show substantial decreases in glucose transporter GLUT4 levels but maintain normal glucose homeostasis. J Biol Chem. 2002; 277:17677–17686. [PubMed: 11884418]

Khan AH, Capilla E, Hou JC, Watson RT, Smith JR, Pessin JE. Entry of newly synthesized GLUT4 into the insulin-responsive storage compartment is dependent upon both the amino terminus and the large cytoplasmic loop. J Biol Chem. 2004; 279:37505–37511. [PubMed: 15247212]

Klausner RD, Donaldson JG, Lippincott-Schwartz J. Brefeldin A: insights into the control of membrane traffic and organelle structure. J Cell Biol. 1992; 116:1071–1080. [PubMed: 1740466]

Klumperman J, Kuliawat R, Griffith JM, Geuze HJ, Arvan P. Mannose 6-phosphate receptors are sorted from immature secretory granules via adaptor protein AP-1, clathrin, and syntaxin 6-positive vesicles. J Cell Biol. 1998; 141:359–371. [PubMed: 9548715]

Kono-Sugita E, Satoh S, Suzuki Y, Egawa M, Udaka N, Ito T, Sekihara H. Insulin-induced GLUT4 recycling in rat adipose cells by a pathway insensitive to brefeldin A. Eur J Biochem. 1996; 236:1033–1037. [PubMed: 8665891]

Kramer HF, Witczak CA, Taylor EB, Fujii N, Hirshman MF, Goodyear LJ. AS160 regulates insulin- and contraction-stimulated glucose uptake in mouse skeletal muscle. J Biol Chem. 2006; 281:31478–31485. [PubMed: 16935857]

Kuliawat R, Kalinina E, Bock J, Fricker L, McGraw TE, Kim SR, Zhong J, Scheller R, Arvan P. Syntaxin-6 SNARE involvement in secretory and endocytic pathways of cultured pancreatic beta-cells. Mol Biol Cell. 2004; 15:1690–16701. [PubMed: 14742717]

Lalioti V, Vergarajauregui S, Sandoval IV. Targeting motifs in GLUT4. Mol Membr Biol. 2001; 18:257–265. [PubMed: 11780754]

Lampson MA, Racz A, Cushman SW, McGraw TE. Demonstration of insulin-responsive trafficking of GLUT4 and vpTfR in fibroblasts. J Cell Sci. 2000; 113:4065–4076. [PubMed: 11058093]

Larance M, Ramm G, Stockli J, van Dam EM, Winata S, Wasinger V, Simpson F, Graham M, Junutula JR, Guilhaus M, et al. Characterization of the role of the Rab GTPase-activating protein AS160 in insulin-regulated GLUT4 trafficking. J Biol Chem. 2005; 280:37803–37813. [PubMed: 16154996]

Li LV, Kandror KV. Golgi-localized, gamma-ear-containing, Arf-binding protein adaptors mediate insulin-responsive trafficking of glucose transporter 4 in 3T3-L1 adipocytes. Mol Endocrinol. 2005; 19:2145–2153. [PubMed: 15774496]

Liu G, Hou JC, Watson RT, Pessin JE. Initial entry of IRAP into the insulin-responsive storage compartment occurs prior to basal or insulin-stimulated plasma membrane recycling. Am J Physiol Endocrinol Metab. 2005; 289:E746–E752. [PubMed: 15928022]

Martin S, Ramm G, Lyttle CT, Meerloo T, Stoorvogel W, James DE. Biogenesis of insulin-responsive GLUT4 vesicles is independent of brefeldin A-sensitive trafficking. Traffic. 2000; 1:652–660. [PubMed: 11208153]

Miinea CP, Sano H, Kane S, Sano E, Fukuda M, Peranen J, Lane WS, Lienhard GE. AS160, the Akt substrate regulating GLUT4 translocation, has a functional Rab GTPase-activating protein domain. Biochem J. 2005; 391:87–93. [PubMed: 15971998]

Min J, Okada S, Coker K, Ceresa BP, Elmendorf JS, Syu LJ, Noda Y, Saltiel AR, Pessin JE. Synip: A novel insulin-regulated syntaxin 4 binding protein mediating GLUT4 translocation in adipocytes. Mol Cell. 1999; 3:751–760. [PubMed: 10394363]

Murray RZ, Wylie FG, Khromykh T, Hume DA, Stow JL. Syntaxin 6 and Vti1b form a novel SNARE complex, which is up-regulated in activated macrophages to facilitate exocytosis of tumor necrosis factor-alpha. J Biol Chem. 2005; 280:10478–10483. [PubMed: 15640147]

Palacios S, Lalioti V, Martinez-Arca S, Chattopadhyay S, Sandoval IV. Recycling of the insulin-sensitive glucose transporter GLUT4. Access of surface internalized GLUT4 molecules to the perinuclear storage compartment is mediated by the Phe5-Gln6-Gln7-Ile8 motif. J Biol Chem. 2001; 276:3371–3383. [PubMed: 11031262]

Peck GR, Ye S, Pham V, Fernando RN, Macaulay SL, Chai SY, Albiston AL. Interaction of the Akt substrate, AS160, with the glucose transporter 4 vesicle marker protein, insulin-regulated aminopeptidase. Mol Endocrinol. 2006; 20:2576–2583. [PubMed: 16762977]

Perera HK, Clarke M, Morris NJ, Hong W, Chamberlain LH, Gould GW. Syntaxin 6 regulates Glut4 trafficking in 3T3-L1 adipocytes. Mol Biol Cell. 2003; 14:2946–2958. [PubMed: 12857877]

Ramm G, Larance M, Guilhaus M, James DE. A role for 14-3-3 in insulin-stimulated GLUT4 translocation through its interaction with the RabGAP AS160. J Biol Chem. 2006; 281:29174–29180. [PubMed: 16880201]

Sano H, Kane S, Sano E, Miinea CP, Asara JM, Lane WS, Garner CW, Lienhard GE. Insulin-stimulated phosphorylation of a Rab GTPase-activating protein regulates GLUT4 translocation. J Biol Chem. 2003; 278:14599–14602. [PubMed: 12637568]

Sano H, Eguez L, Teruel MN, Fukuda M, Chuang TD, Chavez JA, Lienhard GE, McGraw TE. Rab10, a target of the AS160 Rab GAP, is required for insulin-stimulated translocation of GLUT4 to the adipocyte plasma membrane. Cell Metab. 2007; 5:293–303. [PubMed: 17403373]

Satoh S, Nishimura H, Clark AE, Kozka IJ, Vannucci SJ, Simpson IA, Quon MJ, Cushman SW, Holman GD. Use of bismannose photolabel to elucidate insulin-regulated GLUT4 subcellular trafficking kinetics in rat adipose cells. Evidence that exocytosis is a critical site of hormone action. J Biol Chem. 1993; 268:17820–17829. [PubMed: 8349666]

Shewan AM, van Dam EM, Martin S, Luen TB, Hong W, Bryant NJ, James DE. GLUT4 recycles via a trans-Golgi network (TGN) subdomain enriched in Syntaxins 6 and 16 but not TGN38: involvement of an acidic targeting motif. Mol Biol Cell. 2003; 14:973–986. [PubMed: 12631717]

Simonsen A, Gaullier JM, D'Arrigo A, Stenmark H. The Rab5 effector EEA1 interacts directly with syntaxin-6. J Biol Chem. 1999; 274:28857–28860. [PubMed: 10506127]

Steegmaier M, Klumperman J, Foletti DL, Yoo JS, Scheller RH. Vesicle-associated membrane protein 4 is implicated in Trans-Golgi network vesicle trafficking. Mol Biol Cell. 1999; 10:1957–1972. [PubMed: 10359608]

Subtil A, Lampson MA, Keller SR, McGraw TE. Characterization of the insulin-regulated endocytic recycling mechanism in 3T3-L1 adipocytes using a novel reporter molecule. J Biol Chem. 2000; 275:4787–4795. [PubMed: 10671512]

Thong FS, Bilan PJ, Klip A. The Rab GTPase-activating protein AS160 integrates Akt, protein kinase C, and AMP-activated protein kinase signals regulating GLUT4 traffic. Diabetes. 2007; 56:414–423. [PubMed: 17259386]

Ueyama A, Yaworsky KL, Wang Q, Ebina Y, Klip A. GLUT-4myc ectopic expression in L6 myoblasts generates a GLUT-4-specific pool conferring insulin sensitivity. Am J Physiol. 1999; 277:E572–E578. [PubMed: 10484371]

Wang Y, Tai G, Lu L, Johannes L, Hong W, Tang BL. Trans-Golgi network syntaxin 10 functions distinctly from syntaxins 6 and 16. Mol Membr Biol. 2005; 22:313–325. [PubMed: 16154903]

Watson RT, Pessin JE. Functional cooperation of two independent targeting domains in syntaxin 6 is required for its efficient localization in the trans-Golgi network of 3T3L1 adipocytes. J Biol Chem. 2000; 275:1261–1268. [PubMed: 10625671]

Watson RT, Pessin JE. Bridging the GAP between insulin signaling and GLUT4 translocation. Trends Biochem Sci. 2006; 31:215–222. [PubMed: 16540333]

Watson RT, Kanzaki M, Pessin JE. Regulated membrane trafficking of the insulin-responsive glucose transporter 4 in adipocytes. Endocr Rev. 2004a; 25:177–204. [PubMed: 15082519]

Watson RT, Khan AH, Furukawa M, Hou JC, Li L, Kanzaki M, Okada S, Kandror KV, Pessin JE. Entry of newly synthesized GLUT4 into the insulin-responsive storage compartment is GGA dependent. EMBO J. 2004b; 23:2059–2070. [PubMed: 15116067]

Wendler F, Page L, Urbé S, Tooze SA. Homotypic fusion of immature secretory granules during maturation requires syntaxin 6. Mol Biol Cell. 2001; 12:1699–1709. [PubMed: 11408578]

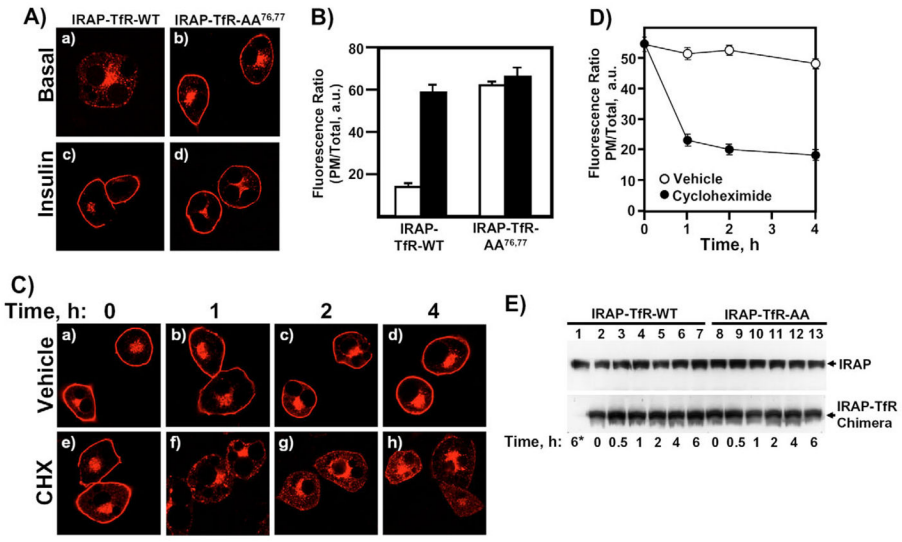

Fig. 1.

Newly synthesized IRAP-TfR-AA^{76,77} defaults to the plasma membrane, where it accumulates under steady-state conditions. (A) Differentiated 3T3L1 adipocytes were electroporated with 50 μg of *IRAP-TfR*-WT (panels a and c) or *IRAP-TfR*-AA^{76,77} (panels b and d) and, 16 hours later, cells were serum-starved and treated without (panels a and b) or with (panels c and d) 100 nM insulin for 20 minutes. The cells were then fixed, permeabilized and labeled with an anti-TfR antibody followed by Texas-Red-conjugated secondary antibody, and were then visualized with a Zeiss LSM510 scanning laser confocal microscope. (B) The data in A were quantified as the ratio of surface fluorescence:total fluorescence, as described in the Materials and Methods. White bars, basal cells; black bars, insulin-stimulated cells. (C) Differentiated 3T3L1 adipocytes were electroporated with 50 μg of *IRAP-TfR*-AA^{76,77} and, 16 hours later, cells were incubated with vehicle alone (panels a–d) or vehicle plus 10 μg/ml cycloheximide (CHX) (panels e–h) for 0, 1, 2 or 4 hours. The cells were then processed for confocal microscopy as indicated in A. (D) The data presented in C were quantified by calculating the ratio of plasma membrane:total fluorescence, as described under Materials and Methods. Results are from three independent experiments, with fifteen cells per experiment (mean ± s.e.m.). (E) Fully differentiated 3T3L1 adipocytes were transfected with 50 μg *IRAP-TfR*-WT or 50 μg *IRAP-TfR*-AA^{76,77} cDNA. After an overnight recovery period, cells were incubated for 0, 0.5, 1, 2, 4 or 6 hours in 10 μg/ml CHX. In lane 1, cells were plated immediately in CHX after electroporation and were then incubated for 6 hours. At the indicated time points, cell lysates were prepared and subjected to western blotting. An anti-IRAP antibody was used to detect both endogenous IRAP (upper panel) and the expressed IRAP-TfR chimera (lower panel). a.u., arbitrary units.

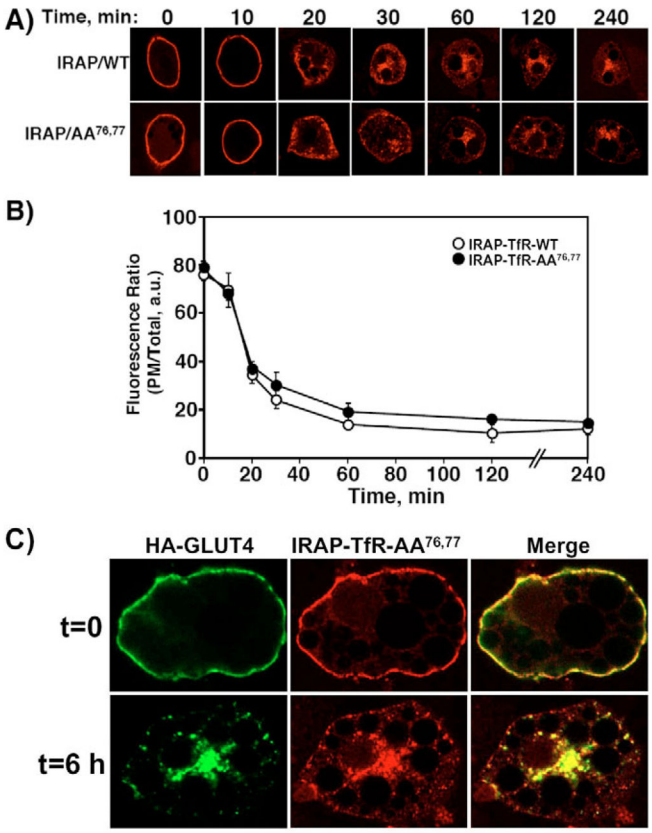

Fig. 2.

IRAP-TfR-AA^{76,77} displays a normal rate and extent of plasma membrane endocytosis. Differentiated 3T3L1 adipocytes were transfected with 50 μg of *IRAP-TfR*-WT or *IRAP-TfR*-AA^{76,77} and, 16 hours later, stimulated with 100 nM insulin (this is only necessary to induce TfR-IRAP-WT translocation but was done for both constructs for internal consistency). The cells were then cooled to 4°C and the cell surface was labeled with the anti-TfR antibody. The cells were washed and warmed to 37°C for various times, as indicated. The cells were then fixed, permeabilized and labeled with Texas-Red-conjugated anti-TfR antibody. (A) Representative cell images are shown. (B) The percentage of cell-surface signal was calculated using the Zeiss LSM 510 software package (mean ± s.e.m. of three independent experiments). (C) Fully differentiated 3T3L1 adipocytes were co-electroporated with 50 μg of both *HA-GLUT4* and *IRAP-TfR*-AA^{76,77}, and were allowed to recover overnight. Cells were then stimulated with 100 nM insulin for 20 minutes, and then surface-labeled on ice with a mouse monoclonal anti-TfR antibody and a polyclonal rabbit HA antibody for 60 minutes. After extensive washing with ice-cold PBS, cells were either fixed in paraformaldehyde (*t*=0) or were warmed to 37°C for 6 hours (*t*=6 h), fixed and labeled with Texas-Red-conjugated donkey anti-mouse and Alexa-Fluor-488-conjugated donkey anti-rabbit secondary antibodies. Images were collected on a Zeiss LSM 510 META confocal microscope. a.u., arbitrary units.

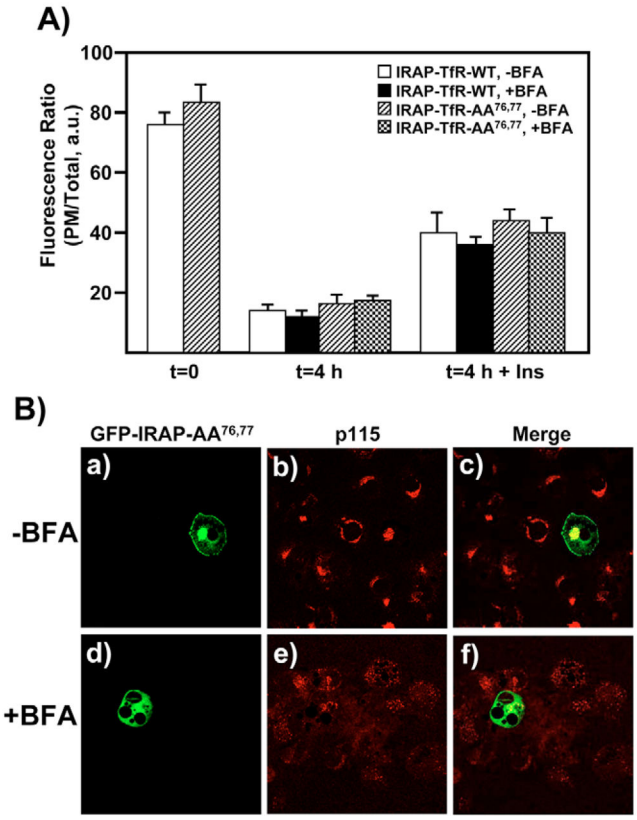

Fig. 3.

IRAP-TfR-WT and IRAP-TfR-AA^{76,77} both recycle from the cell surface back to an IRC that is BFA-insensitive. (A) Fully differentiated 3T3L1 adipocytes were transfected with 50 μg of either *IRAP-TfR*-WT or *IRAP-TfR*-AA^{76,77} and, 16 hours later, cells were stimulated with insulin and surface-labeled with the anti-TfR antibody on ice for 60 minutes. Cells were then washed with PBS and incubated at 37°C for 4 hours. For the BFA treatment, cells were incubated with BFA (5 μg/ml) during the last 30 minutes of the washout period and also during the second round of insulin treatment. Control cells were incubated with vehicle alone. Following the second round of treatment without or with insulin (100 nM, 30 minutes), cells were fixed, permeabilized and labeled with Texas-Red-conjugated secondary antibody, as described under Materials and Methods. The ratio of plasma membrane fluorescence:total fluorescence was determined using the Zeiss LSM software package (mean ± s.e.m. of three independent experiments). (B) Control experiments demonstrating the efficacy of 5 μg/ml BFA. Cells were transfected with 50 μg of *GFP-IRAP*-AA^{76,77} reporter construct and immediately plated in media either without (panels a-c) or with (panels d–f) 5 μg/ml BFA. After a 3-hour recovery period, cells were fixed and labeled with an anti-p115 monoclonal antibody, followed by Texas Red secondary antibody. a.u., arbitrary units.

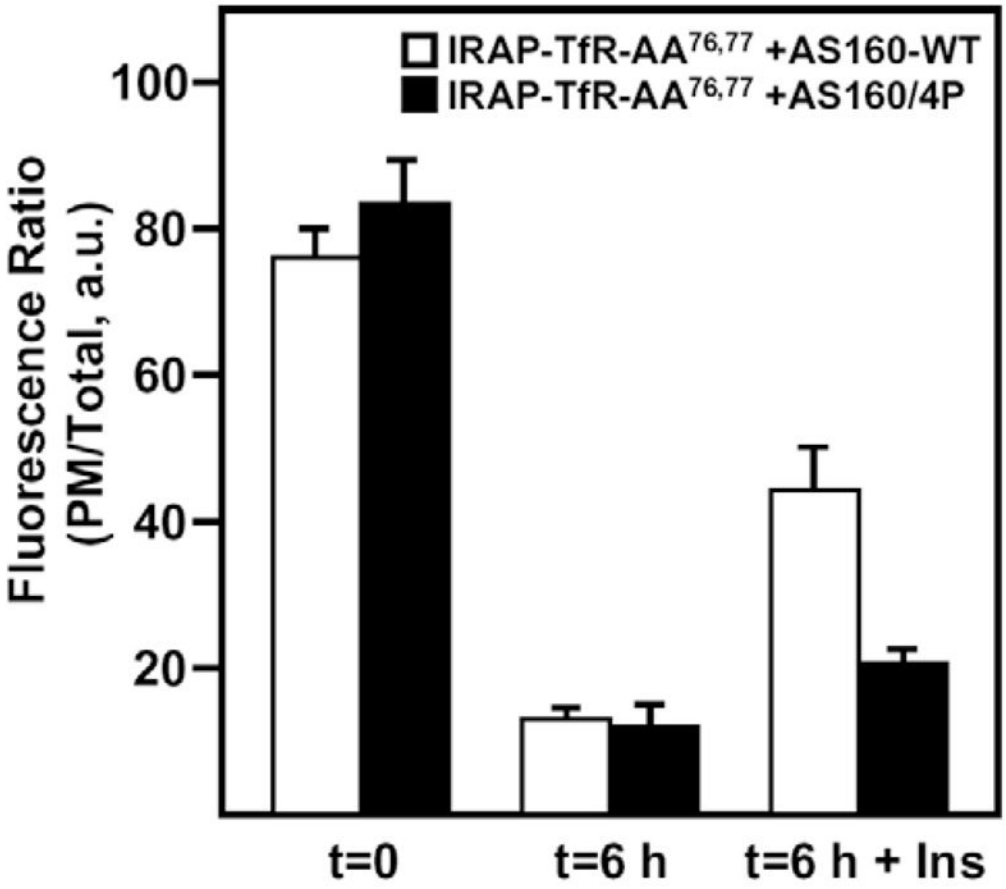

Fig. 4.

A dominant-interfering mutant form of AS160 (AS160-4P) inhibits the insulin-stimulated exit of IRAP-TfR-AA^{76,77} from the IRC following endocytosis from the cell surface. Fully differentiated 3T3L1 adipocytes were electroporated with 50 μg of *IRAP-TfR*-AA^{76,77} and either *AS160*-WT (white bars), or *AS160*-4P (black bars). Following a 16-hour recovery period, cells were surface-labeled with the anti-TfR antibody on ice for 60 minutes. Cells were then warmed to 37°C for 6 hours to allow endocytosis to occur, then treated without or with 100 nM insulin for 30 minutes, fixed, permeabilized and labeled with Texas-Red-conjugated secondary antibody as described under Materials and Methods. The ratio of plasma membrane fluorescence to total fluorescence was determined using the Zeiss LSM software package (mean ± s.e.m. of three independent experiments). a.u., arbitrary units.

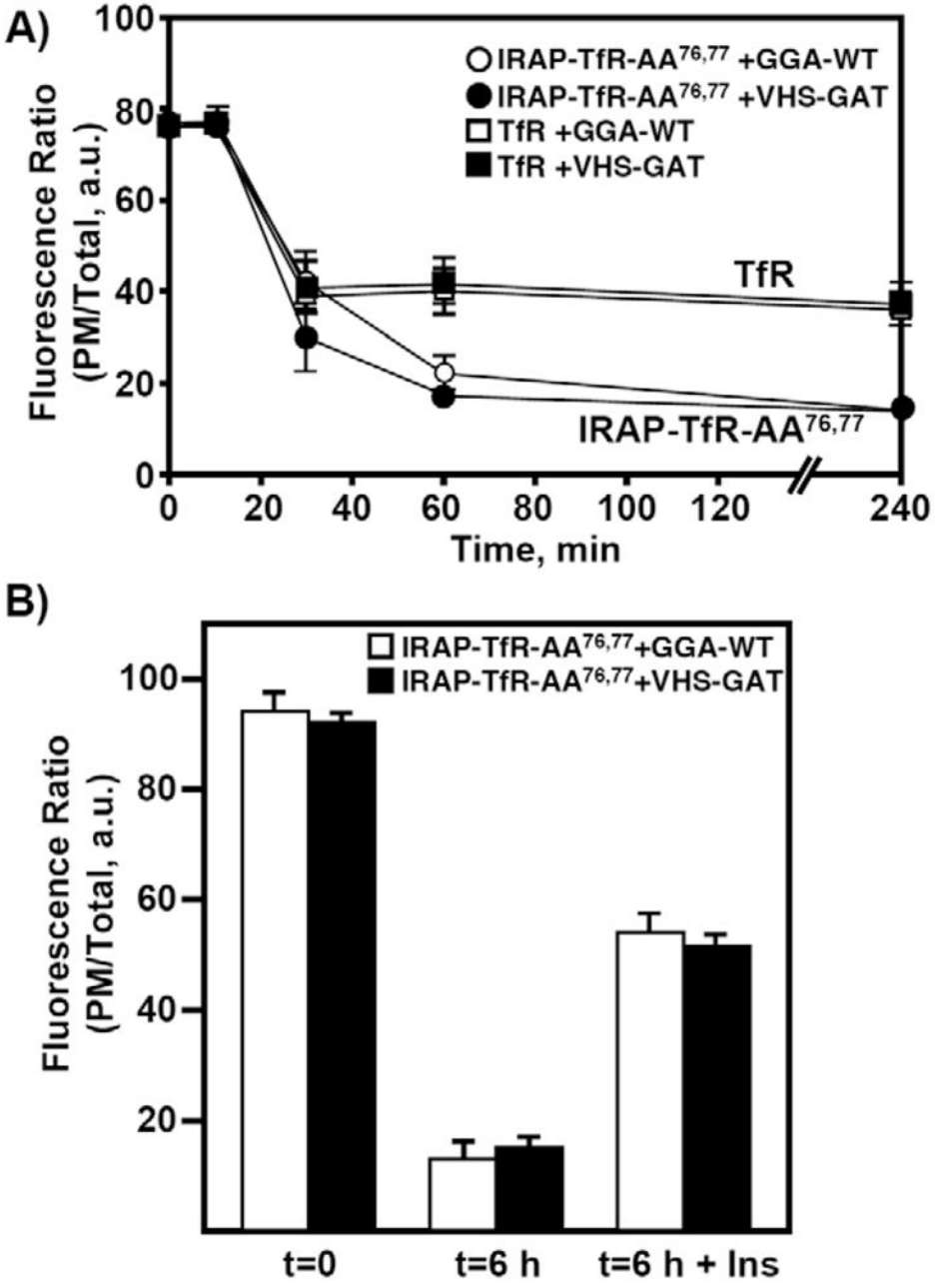

Fig. 5.

GGA clathrin adaptors function specifically during the biosynthetic entry of IRAP into the IRC. (A) Fully differentiated 3T3L1 adipocytes were transfected with 50 μg of *IRAP-TfR*-WT or *IRAP-TfR*-AA^{76,77} and, 16 hours later, were stimulated with 100 nM insulin. Following surface labeling with the anti-TfR antibody, endocytosis time courses were performed as described in Fig. 1 and in the Materials and Methods. (B) Fully differentiated 3T3L1 adipocytes were electroporated with 50 μg of *IRAP-TfR*-AA^{76,77} and 200 μg of either *GGA*-WT or *VHS-GAT*. After an overnight recovery, cells were surface-labeled with the anti-TfR antibody as described in Fig. 3 and in the Materials and Methods. Following a 6-

hour washout period at 37°C, cells were treated without or with 100 nM insulin for 30 minutes, fixed, permeabilized and labeled with Texas-Red-conjugated secondary antibody as described under Materials and Methods. The ratio of plasma membrane fluorescence to total fluorescence was determined using the Zeiss LSM software package (mean ± s.e.m. of three independent experiments). a.u., arbitrary units.

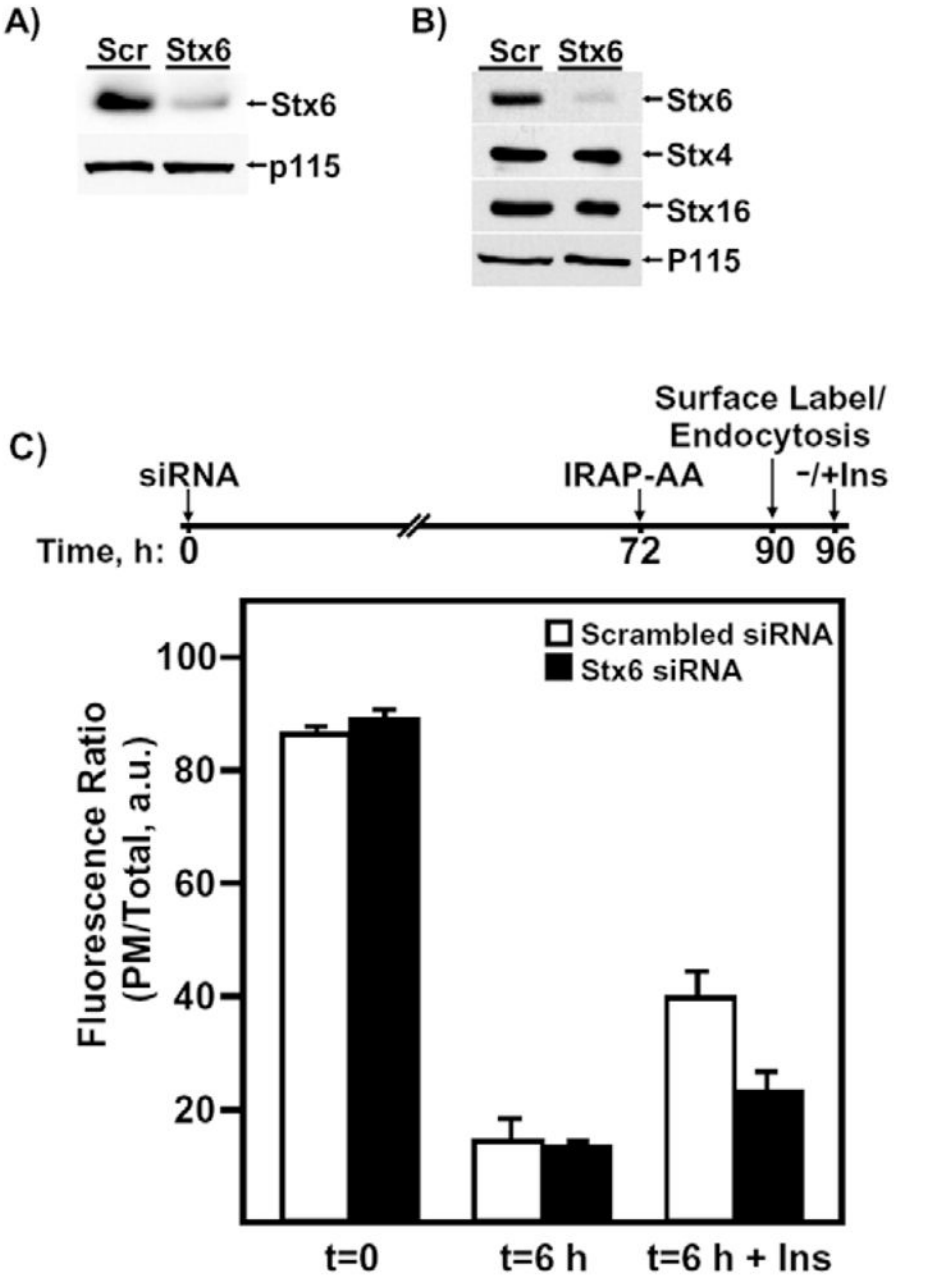

Fig. 6.

Stx6 functions during the re-entry of IRAP into the IRC following endocytosis from the cell surface. (A) Western blot showing the extent of Stx6 knockdown by siRNA (5 nmol) 72 hours after transfection. (B) Western blot showing the extent and specificity of Stx6 knockdown by siRNA (5 nmol) 96 hours after transfection. Lane 1, scrambled-siRNA-transfected cells; lane 2, *Stx6*-siRNA-transfected cells. For the 96-hour time point, the same membrane was stripped and re-probed with anti-Stx4, -Stx16 and -p115 antibodies. p115 is a Golgi-tethering factor and is used here as a protein loading control. (C) Cells were transfected with either 5 nmol of scrambled or *Stx6* siRNA and, 72 hours later, were

transfected with *IRAP-TfR*-WT reporter. Following an 18-hours recovery period, cells were stimulated with insulin and surface-labeled on ice with the anti-TfR monoclonal antibody. Following a 6-hour washout period at 37°C, cells were re-stimulated with or without insulin, fixed, labeled with Texas-Red-secondary antibody and processed for confocal microscopy (mean ± s.e.m. of three independent experiments). A timeline for the transfections is shown above the bar graph for clarity. a.u., arbitrary units.

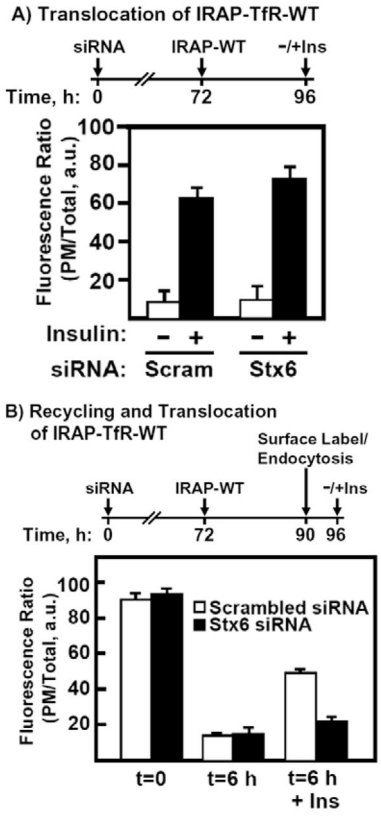

Fig. 7.

Stx6 function is not required for the insulin-stimulated exit of IRAP from the IRC. (A) Fully differentiated 3T3L1 adipocytes were transfected with 5 nmol of scrambled or *Stx6* siRNA and, 72 hours later, were transfected with 50 μg *EGFP-IRAP-TfR*-WT reporter. Following a 24-hour recovery period, cells were treated with or without insulin, fixed and labeled with Texas Red secondary antibody. The ratio of plasma membrane to total fluorescence was determined using Zeiss LSM software. (B) Cells were transfected with either 5 nmol of scrambled or *Stx6* siRNA and, 72 hours later, were transfected with *IRAP-TfR*-WT reporter. Following an 18-hour recovery period, cells were stimulated with insulin and surface-labeled on ice with anti-TfR monoclonal antibody. Following a 6-hour washout at 37°C, cells were re-stimulated with or without insulin, fixed, labeled with Texas Red secondary antibody and processed for confocal microscopy (mean ± s.e.m. of three independent experiments). A timeline for the transfections is shown above the bar graphs for clarity. Scram, scrambled siRNA. a.u., arbitrary units.